Steel and Composite Structures, *Vol. 22, No. 5 (2016) 1039-1054*
DOI: http://dx.doi.org/10.12989/scs.2016.22.5.1039

Dynamic characteristics and wind-induced vibration coefficients of purlin-sheet roofs

Yingying Zhang [*1], Xiaoguang Song [2b] and Qilin Zhang [3c]

[1] *State Key Laboratory for GeoMechanics and Deep Underground Engineering, Jiangsu Key Laboratory of Environmental Impact and Structural Safety in Engineering, China University of Mining and Technology, Xuzhou Jiangsu, 221116, China*
[2] *Shandong Academy of building research, Jinan Shandong, 250031, China*
[3] *College of Civil Engineering, Tongji University, Shanghai 200092, China*

(*Received April 18, 2016, Revised November 07, 2016, Accepted November 10, 2016*)

Abstract. This paper presents the dynamic characteristics analysis of the purlin-sheet roofs by the random vibration theories. Results show that the natural vibration frequency of the purlin-sheet roof is low, while the frequencies and mode distributions are very intensive. The random vibration theory should be used for the dynamic characteristics of the roof structures due to complex vibration response. Among the first 20th vibration modes, the first vibration mode is mainly the deformations of purlins, while the rest modes are the overall deformations of the roof. In the following 30th modes, it mainly performs unilateral local deformations of the roof. The frequency distribution of the first 20th modes varies significantly while those of the following 30th modes are relatively sensitive. For different parts, the contributions of vibration modes on the vibration response are different. For the part far from the roof ridge, only considering the first 5th modes can reflect the wind-induced vibration response. For the part near the ridge, at least the first 12 modes should be considered, due to complex vibration response. The wind vibration coefficients of the upwind side are slightly higher than that of the leeward side. Finally, the corresponding wind vibration coefficient for the purlin-sheet roof is proposed.

Keywords: purlin sheet roof; random vibration theory; dynamic characteristic; wind-induced vibration coefficient

1. Introduction

Compared with traditional roof structures, the thin-walled purlin-sheet roof is more sensitive to the wind loads, due to large-span, low slope, low natural frequency and uneven stiffness and mass (Zhu *et al*. 2014, Zhang and Tong 2016). Those low structures always locate in the regions with high turbulence degree and wind velocity variations (Habte *et al*. 2015, Lovisa *et al*. 2013). The destruction of lower houses always starts from the surface cladding system, especially the roof. The wind field of roof structures has significant three-dimensional characteristics and the flow field characteristic is quite complicated. It is easy to observe the flow separation, reattachment, and the vortex shedding phenomenon of tail structures. There are many researches on the static behaviors of suspension roof, flat roof, sloping roof and spherical roof (Cai *et al*. 2013a, b, Yuan *et*

*Corresponding author, Ph.D., E-mail: zhangyingying85@163.com

 ISSN: 1229-9367 (Print), 1598-6233 (Online)

al. 2014, Krentowski 2014). The geometry of the roof system has great effects on the distribution of wind pressure on the roof. Even if the shape of the roof is similar, the differences of local structures for example, cornice, parapet and roof slope, will lead to the differences of local or overall pressure distributions. Therefore, it is necessary to study the dynamic characteristics and wind vibration coefficient of thin-walled purlin-sheet roof structures.

Flat roofs or small curvature roofs are the most common forms of lightweight steel roof (Cai *et al*. 2013c, d). Uematsu *et al*. (1997, 1999) studied the design wind loads of circular flat roof and proposed a simplified formula to evaluate the design wind load of long-span flat roofs, based on the dynamic response of the turbulence wind load. The sloping roof is a typical low-rise and large-span structural form, of which the pressure distribution is related with slope angle and wind orientation angle. For common low-slope roofs, the forming of the wind suction in the roof is because of flow separation near the cornice, ridge and edge of the roofs. With roof slope and wind direction changing, the status of airflow separation and the distribution & size of the roof suction changes. When the roof angle increases from 15° to 20°, the wind pressure coefficient on the windward side decreases significantly, and the distribution tends to be uniform. When the roof angle increases from 20° to 30°, the positive pressure appears in the windward side, and no significant changing appears in the leeward of the roof (Martins *et al*. 2016, Liu *et al*. 2016).

There are some researches on the wind pressure characteristics of flat roofs, especially for the corners of the roofs with high wind pressure distribution (Zhu 2014, Cai *et al*. 2015). Tieleman *et al*. (1994) proposed a formula of wind pressure coefficient to describe the distributions of mean pressure, fluctuating pressure and the critical pressure. Lin *et al*. (1995) found that the distribution of wind pressure in the surface can be described by the dimensionless coordinate and proposed the critical pressure regarding to different wind directions. Lou *et al*. (2002) proposed that the wind can produce the separation and re-attachment of complex flows in the large-span roof and used the partition method to describe the wind pressure coefficient.

Now, there are three main methods of wind loads research include field measurement, wind tunnel model test and computational fluid dynamics (CFD). The field measurement is always to obtain the first-hand wind characteristics and structural response by the sensors of wind velocity, and accelerometer instruments, etc. It is an effective way to study the structural response, but huge cost and various uncontrolled factors limit its applications in practical engineering (Robertson *et al*. 1998, Tamura 1999, Xu *et al*. 2010).

The wind tunnel test, also known as “physical wind tunnel test”, is to simulate actual wind environment and actual buildings in the atmosphere boundary layer (Ahmad and Kumar 2002, Ginger 2004, Habte *et al*. 2015). Cope (Cope *et al*. 2005) studied the effects of distributions and probability characteristics of wind pressure of the roof sheets in typical low-rise hyperboloid buildings and compared with the ASCE codes 7-98 and the experiment data. Farquhar and Kopp (2005) carried the uniform static loading and wind tunnel tests of 1:25 scaled roofs with slippable clips and compared with the loading capacity of full size models of the Mississippi State University, in which the relationship between the static and dynamic loading bearing capacities of roof sheets were discussed. Surry *et al*. (2007) carried out the full-size tests to simulate the wind loads on the roof with slippable clips in the Mississippi State University and found that the response surface method is an effective way to calculate the wind pressure.

With rapid development of computer hardware and computational fluid dynamics, the numerical wind tunnel method is more popular in the wind-induced response analysis (Sun *et al*. 2008, Zhou *et al*. 2014, 2015). It is to apply the computational fluid dynamics to simulate the changing of surrounding wind field and obtain the distributions of the surface wind loads.

Compared with traditional wind tunnel methods, the numerical method is more popular for many advantages, including high calculation efficiency, parametric analysis and low cost, et al.

In the wind-induces response analysis, there are three analysis methods, including the analytical method, the discrete frequency domain method, and the discrete time domain method (Lovisa *et al*. 2013, Jacklin *et al*. 2014, Jubayer and Hangan 2014). For simple structures whose first mode is the dominant, the wind loads can be approximately equivalent to the definite static load. Meanwhile, the fluctuating wind is random and its vibration response can be solved by the random vibration theory (Huang and Wang 2008). However, the analytical method is only limited to some specific structural forms, which cannot meet the increasing requirements of complex practical engineering problems.

The time domain method is to calculate the dynamic response of the structures by the progressive integral method, based on the time history of wind loads. It can be used for the analysis of linear and nonlinear structures with high accuracy. Until now, there are not enough records about the field measurement of the time history of wind velocity (Li and Dong 2001). Relatively, the time history diagrams of wind velocity based on the numerical simulation method is a very effective method to study the wind-induced vibration response, widely used in the practical engineering.

The frequency domain method is proposed based on the random vibration theory, in which the relationship between the power spectrum of displacement response and fluctuating wind load is built. Its higher computational efficiency can directly obtain the basic characteristics of wind-induced structural response. Nakayama *et al*. (1998) pointed out that the some high-order modes are always ignored in the analysis of large-span roof structures and it should be implemented to calculate the static displacement. Lu *et al*. (2002) found that the vertical vibration response of large-span flat roofs is mainly dominated by the first order mode, and the effects of higher order modes on the vertical vibration response of roof sheets are very small. The roof stiffness and the wind velocity have significant effects on the vertical vibration response of large span flat roof, but slight effects on the wind vibration coefficient of structural displacement. Fu *et al*. (2010) studied the wind-induced displacement response of roof structures in Guangzhou International Convention and Exhibition Center and proposed the method to identify the natural vertical frequency of large-span roof structures.

There are two main numerical simulation method for wind velocity time history, including the spectrum method and the linear filtering method. Shu and Zhou (2003) used the Auto-Regressive (AR) model to simulate the time history of randomly fluctuating winds, and found that the AR model can effectively simulate the time history of fluctuating wind by considering time correlation and space correlation. Kasperski (2009) proposed that the resonance effect should be considered in the design due to high strength building envelope and nonlinear analysis. Generally, for the large span roof structures whose natural vibration period is higher than 0.25 s, the wind-induced vibration is obvious and it increases with the natural vibration period increasing (Huang and Wang 2008).

This paper aims to present the dynamic characteristics analysis and wind-induced vibration coefficients of purlin-sheet roofs by the random vibration theories. First, the research methods and analysis theories/models for the wind-induced vibration response of the purlin-sheet roofs are discussed. Then, the dynamic response of purlin-sheet roofs are studied by the random vibration theories. Finally, the wind vibration coefficients of the purlin-sheet roofs are proposed. This paper can be references for the wind-induced response analysis of purlin-sheet roofs.

2. Materials and methology

The typical single-span purlin-sheet roof is taken as the research object. The dimensions of the roof structures are shown in Table 1 and Fig. 1. The mass of the wall beam and the panels are applied as uniform loads and the distances between the wall beams are 1.5 m. The wind vibration response of the structure are not only related to the fluctuation characteristics of the wind, but also to the natural characteristics of the structure. Therefore, the natural vibration characteristics of roof structures should be studied, including natural vibration frequency and modes. The modal analysis of the purlin-sheet roof is carried out and the first 50 order modes and natural frequencies are obtained.

The frequency domain method is conduced to describe the dynamic displacement by the linear combinations of the generalized coordinates in different modes and the fundamental modes in the modal space. The approximate analysis method of Davenport spectrum is always conducted in the analysis. The random vibration theories are used to analyze the power spectrum density of wind loads. For large-span purlin-sheet roof, the first order mode may not be the dominant mode and the effects of multi-modes should be considered in the wind-induced vibration analysis. Considering that not all the modes have the same effects on the structural dynamic response, so it is not necessary to include all the generalized coordinates in all modes. Therefore, some important and necessary modes should be chosen for the wind-induced vibration analysis. The participation contributions of the modes can be evaluated by the proportions of strain energy in the total strain energy. The detailed calculation model can be seen in Section 3.2.2, in which the effect of vibration mode on the structural response and the mode combinations are analyzed.

The wind-induced vibration coefficients of the purlin-sheet roofs are obtained based on the random vibration theories. The first 20 vibration modes are chosen to analyze the participation

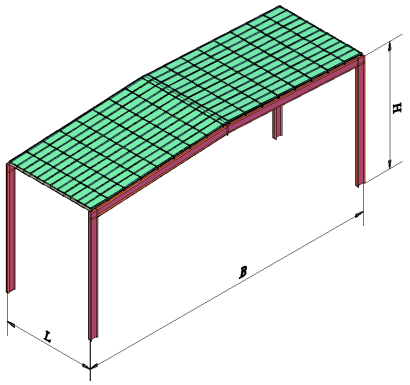

Fig. 1 Dimensions of single-span purlin-sheet roof

Table 1 Single span cold-formed purlins plate roof structure parameters

Corrugated sheet type	Purlin type	Connection type	Roof slope *i*	Purlin span *L* (m)	Frame span *B* (m)	Eaves height *H* (m)	Purlin spacing *S* (m)
YW25-1000	Z180×2.5	Self-drilling screws	5%	7.5	24	10	1.5

ratio and the wind-induced vibration coefficient. The wind-induced vibration force can be obtained based on the displacement of nodes. The wind-induced vibration coefficient of the roof structure can be calculated according to the current design codes (Huang and Wang 2008).

3. Results and discussions

3.1 Dynamic characteristics of cold-formed purlin-sheet roof

Due to the limited layout, part of the vibration modes and natural vibration frequencies of YW25-1000 roof structure are presented in Fig. 2.

From Fig. 2, the participation contribution of portal frame is significant in the first 3nd modes of the roof structure. As shown in Fig. 3(a)-(c), anti-symmetric deformations of two trusses can be observed in the 1st mode, while the symmetrical deformations are observed in the 2nd modes. In the 3rd mode, symmetrical deformations appear in the ridge frame but the deformations of steel beams are anti-symmetric. In the rest modes, the participation of rigid frame is not significant. In the first 20 vibration modes, the main performance is the deformations of purlins, while the overall deformation of the roof is the dominant. In the next 30 vibration modes, local deformation is the

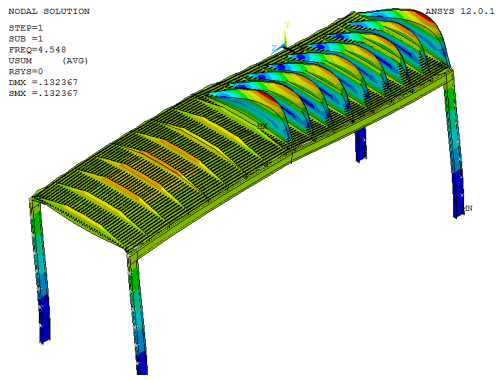

1st mode (f_1 = 4.548 Hz)

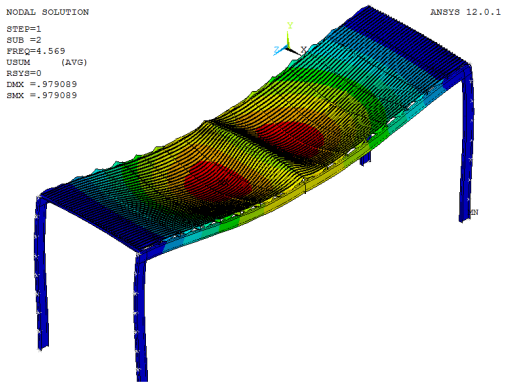

2nd mode (f_2 = 4.569 Hz)

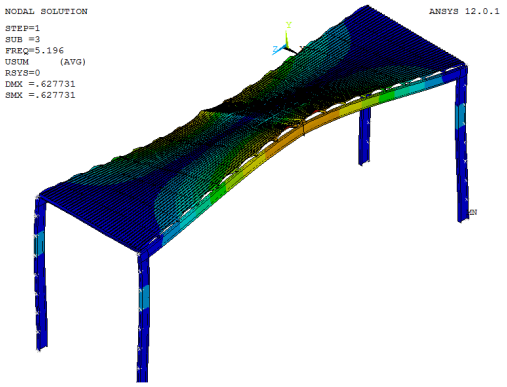

3rd mode (f_3 = 5.196 Hz)

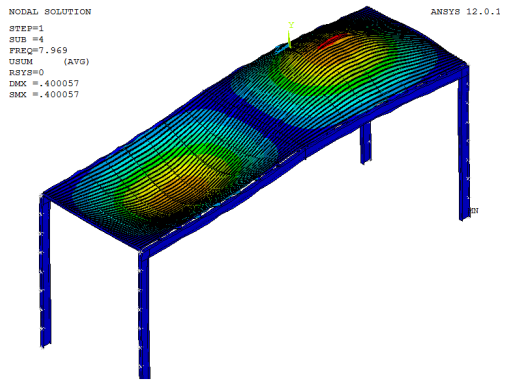

4th mode (f_4 = 7.969 Hz)

Fig. 2 Vibration modes of YW25-1000 roof

dominant.

The distributions of the first 50th modal frequencies of the roof structure are shown in Fig. 4. The frequencies of the first 20th modes (overall mode) are different, while the following 30th modes (local mode) are similar.

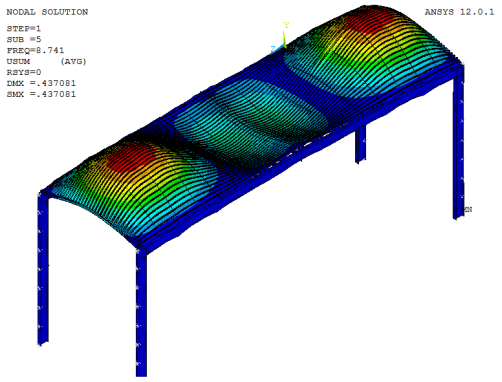

5th mode (f_5 = 8.741 Hz)

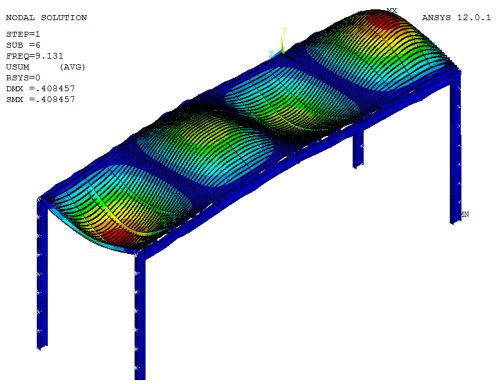

6th mode (f_6 = 9.131 Hz)

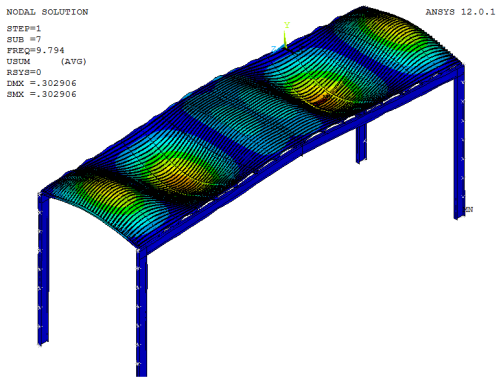

7th mode (f_7 = 9.794 Hz)

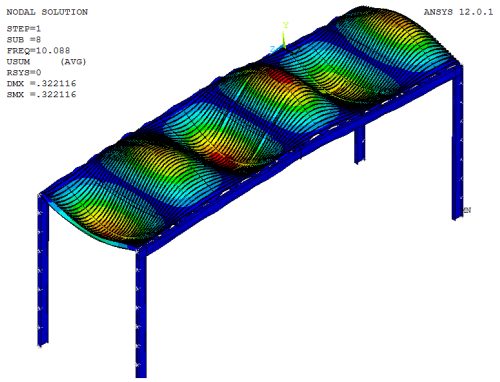

8th mode (f_8 = 10.088 Hz)

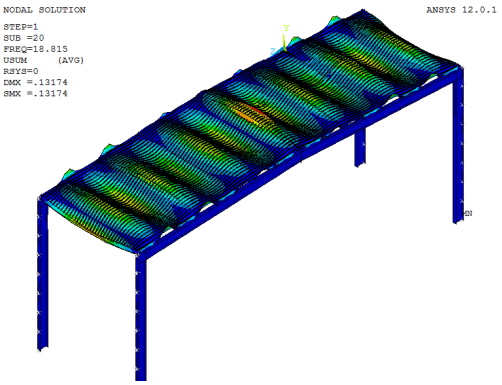

20th mode (f_{20} = 18.815 Hz)

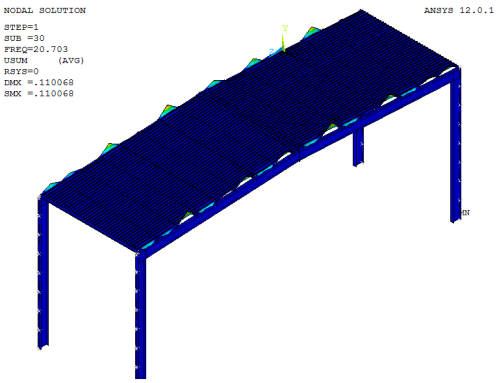

30th mode (f_{30} = 20.703 Hz)

Fig. 2 Continued

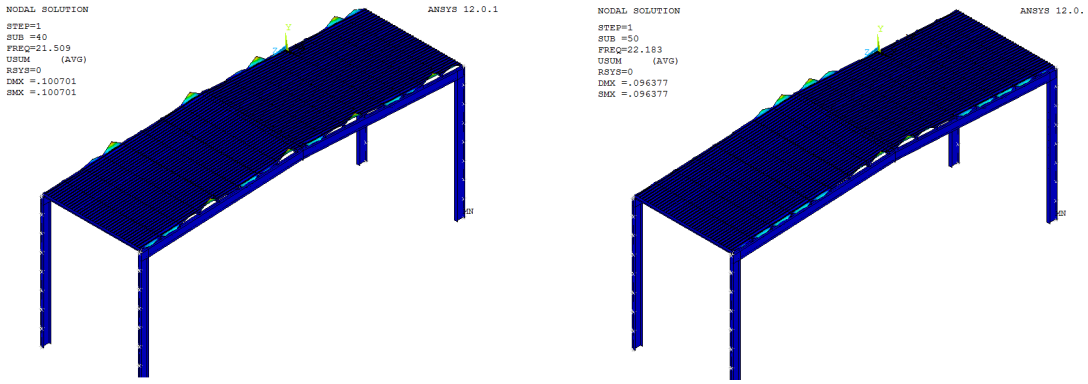

40th mode (f_{40} = 21.509 Hz) 50th mode (f_{50} = 22.183 Hz)

Fig. 2 Continued

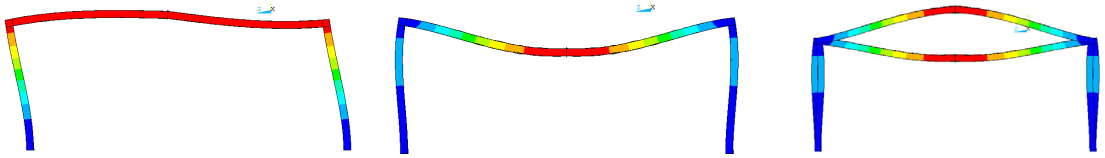

(a) 1st order vibration mode (b) 2nd order vibration mode (c) 3rd order vibration mode

Fig. 3 First three modes of frame vibrations

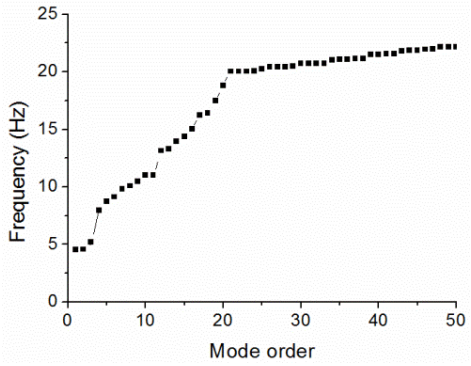

Fig. 4 Frequencies of first 50th orders modes

The dynamic characteristics analysis shows that the fundamental natural vibration period T_1 of the roof structure is 0.22 s. According to the GB50009-2012 (2002), for the high-rise buildings whose fundamental natural period is less than 0.25 s, the wind vibration effect is generally slight and can be ignored in the approximate analysis of wind-induced effects. However, different from high-rise buildings, the purlin-sheet roofs perform light weight, large flexibility and small damping. It determines that the natural vibration frequency is low and the frequencies and mode distributions are very intensive. Then, the wind vibration response of the roof structure is very complex. Therefore, the random vibration theory should be employed to analyze the effect of

fluctuating winds on the dynamic characteristics of the roof structures.

3.2 Analysis of the participation contributions of vibration modes based on the random vibration theories

3.2.1 Dynamic spectrum of fluctuating winds

There are many types of wind spectrums based on the experiment data. In most of wind spectrums, the wind velocity varies along the height, such as Karman turbulent wind velocity spectrum, Simiu fluctuating wind velocity spectrum, and Hino fluctuating wind velocity spectrum. In some wind spectrums, the wind velocity remains unchanged along the height, such as Davenport fluctuating wind velocity spectrum (Davenport 1967) and Harris fluctuating wind velocity spectrum.

Davenport proposed the empirical expressions according to more than 90 measurements in different locations and heights in the world. The turbulence integral length scale L in the horizontal gust spectrum is assumed as a constant. The fluctuating wind spectrum is considered as the mean measured values of different heights (Huang and Wang 2008)

$$\frac{nS_v(n)}{\bar{v}_{10}^{-2}} = \frac{4kx^2}{(1+x^2)^{4/3}} \tag{1}$$

where, $x = 1200\dfrac{n}{\bar{v}_{10}}$, $\bar{v}_{10}$ is the mean wind velocity at the standard height of 10 m (m/s) , n is the frequency of fluctuating wind (Hz), and k is the surface roughness coefficient.

Although the velocity spectrum varied along the height seems more reasonable, its calculated structural response is very close to the results by Davenport spectrum. The deviations are less than 5%, and most of them are between 1-3% (Zhang 2006). Therefore, the Davenport spectrum is widely conducted as the approximate analysis method, just as shown in many specifications. On the other hand, the Davenport spectrum contains the spectral data of more than 90 areas around the world. Finally, after comprehensive consideration, the Davenport spectrum is employed in this analysis.

3.2.2 The random vibration theories on the wind-induced structural response

The motion equation of the structures with N degrees of freedom is as follow.

$$M\ddot{y}(t) + C\dot{y}(t) + Ky(t) = P_f(t) \tag{2}$$

where, M is the mass of the structure, C is the damping coefficient, and K is the stiffness matrices. $\ddot{y}(t), \dot{y}(t), y(t)$ are the wind acceleration, wind velocity and displacement vector, respectively. $P_f(t)$ is the vector of fluctuating wind.

$$y_i(t) = \sum_{j=1}^{n} \phi_{ji} q_j(t) \tag{3}$$

where, ϕ_{ji} is the vibration coefficient of mode j for node i and $q_j(t)$ is the generalized coordinate of mode j. Based on the assumption that Rayleigh Damping meets the orthogonally, the motion equations can be got by incorporating the Eq. (3) into Eq. (2), as follows

$$\begin{aligned}
&\ddot{q}_j(t)+2\zeta_j\omega_j\dot{q}(t)+\omega_j^2 q(t)=F_j(t)=\frac{P_{fj}^* f(t)}{M_j^*}\\
&P_{fj}^*=\sum_i w_{fi}A_i\phi_{ji}\quad (j=1,2,3,\cdots,n)\\
&M_j^*=\sum_i M_i\phi_{ji}^2
\end{aligned}\tag{4}$$

where, ω_j and ζ_j are the natural frequency and damping ratio of vibration mode j, $F_j(t) \times M_j^*$ is the generalized force of mode j corresponding to the fluctuating wind. After separating the time component, P_{fj}^* is the generalized force of mode j corresponding to the static wind load. w_{fi} is the fluctuating surface force of node i, A_i is the related area of node i, $f(t)$ is the time function of fluctuating wind, and M_j^* is the generalized mass of mode j.

Because the time function $f(t)$ of the fluctuating wind is random, the equation (4) should be solved based on the random vibration theory. The power spectrum density $S_f(z, \omega)$ is the representative input data, where z is the height and ω is the circular frequency of the fluctuating wind. The spatial correlation coefficient $\rho_{i,i'}(\omega)$ should be considered because of the spatial correlation of fluctuating winds. Meanwhile, the power spectral density $S_Y(z_i, \omega)$ is the representative output data. Therefore, the root variance σ_{yi} of the dynamic displacement response in node i is as follows.

$$\begin{aligned}
\sigma_{yi}&=\sqrt{\int_{-\infty}^{\infty}S_Y(z_i,\omega)d\omega}=\sqrt{\sum_{j=1}^{n}\sigma_{yji}^2}\\
&=\sqrt{\sum_{j=1}^{n}\phi_{ji}^2\int_0^H\int_0^H\int_{-\infty}^{\infty}\sqrt{S_{F_jF_j}(z,\omega)S_{F_jF_j}(z',\omega)}\left|H_j(i\omega)\right|^2 dzdz'd\omega}\\
&=\sqrt{\sum_{j=1}^{n}\frac{\phi_{ji}^2}{(M_j^*)^2}\int_{-\infty}^{\infty}\sum_i\sum_{i'}\sigma_{wfi}A_i\sigma_{wfi'}A_{i'}\rho_{ii'}(\omega)\phi_{ji}\phi_{ji'}\sqrt{S_f(z_i,\omega)S_f(z_{i'},\omega)}\left|H_j(i\omega)\right|^2 d\omega}
\end{aligned}\tag{5}$$

where, $S_{FjFj}(z_i, \omega)$ is the power spectrum density of mode j for node i due to the fluctuating wind, and $H_j(i\omega)$ is the frequency response function of mode j.

Because the root variance σ_{yi} only present the mean square amplitude, a certain factor (peak factor) μ is introduced to calculate the response amplitude in the condition of certain guaranteed rate, as follows

$$\begin{aligned}
y_i&=\mu\sigma_{yi}=\sqrt{\sum_{j=1}^{n}y_{ji}^2}=\mu\sqrt{\sum_{j=1}^{n}\sigma_{yji}^2}\\
&=\sqrt{\sum_{j=1}^{n}\frac{\phi_{ji}^2}{(M_j^*)^2}\int_{-\infty}^{\infty}\sum_i\sum_{i'}w_{fi}A_iw_{fi'}A_{i'}\rho_{ii'}(\omega)\phi_{ji}\phi_{ji'}\sqrt{S_f(z_i,\omega)S_f(z_{i'},\omega)}\left|H_j(i\omega)\right|^2 d\omega}
\end{aligned}\tag{6}$$

3.2.3 Effect of vibration mode on the structural response and the mode combinations

The natural vibration frequencies of the purlin-sheet roof are very intensive and the shapes of the vibration modes are complex. The 1st mode may not be the dominant, and the effects of multi-modes in the analysis of wind-induced vibrations should be considered. The participation

contributions of the modes can be evaluated by the proportions of strain energy in the total strain energy. However, due to complex vibration response, it is difficult to get the accurate structural response and structural strain energy by considering finite vibration modes. Therefore, the proportion of strain energy of vibration modes should be obtained in order to justify the mode contributions and choose the necessary modes.

As shown in Fig. 2, all the next 30 modes (21st-50th) of the purlin-sheet roof are local deformation modes in a small region of the roof. Therefore, after consideration, the first 20th modes are chosen to analyze the participation ratio and the wind-induced vibration coefficient. The participation ratio of various vibration modes can be obtained according to the strain energy of various modes by the random vibration theory, in order to choose the main vibration modes.

According to the theory of linear random vibration, the generalized force spectrum of i th and j th vibration mode can be obtained as follows.

$$S_{ij}^{*}(n)=\sum_{k=1}^{3N}\sum_{m=1}^{3N}S_{km}(n)\phi_i(k)\phi_j(m)/(M_i^{*}M_j^{*}) \tag{7}$$

where, $\phi_i(k)$ is mode i of node k, $\phi_j(m)$ is mode j of node m; M_i^{*} and M_j^{*} are the generalized mass of mode i and mode j; $S_{km}(n)$ is the value of line k column m in the load spectrum matrix.

The generalized displacement covariance of i th mode and j th mode are as follows

$$\sigma_{ij}^2=\int_0^{\infty}H_i(in)H_j(-in)S_{ij}^{*}(n)dn \tag{8}$$

$$H_i(in)=\frac{1}{\left[(2\pi n_i)^2-(2\pi n)^2+i(2\xi_{ei}(2\pi n_i)(2\pi n))\right]} \tag{9}$$

$$H_j(-in)=\frac{1}{\left[(2\pi n_j)^2-(2\pi n)^2-i(2\xi_{ej}(2\pi n_j)(2\pi n))\right]} \tag{10}$$

where, $H_i(in)$ is the transfer function of mode i, i is the unit of imaginary number, ξ_{ei} is the damping ratio of mode i, and n_i is the frequency of mode i.

The contribution of vibration modes is related with mode displacement and mode energy. In order to analyze the participation ratio of vibration modes on the wind-induced displacement, the covariance matrix of generalized displacement should be calculated. Then, the average strain energy of the fluctuating wind loads for mode j can be obtained as follows.

$$\overline{E}_j=\frac{1}{2}k_j\sigma_{jj}^2=\frac{1}{2}m_j\omega_j^2\sigma_{jj}^2 \tag{11}$$

where, k_j, m_j, ω_j are the generalized stiffness, the generalized mass and circular frequency of mode j, and σ_{jj}^2 is generalized displacement variance of mode j.

The sum of strain energy of the first 20th modes is

$$\overline{E}_{20}=\sum_{j=1}^{20}\overline{E}_j \tag{12}$$

The total energy contribution ratio of mode j is

$$R_{Ej} = \frac{\overline{E}_j}{\overline{E}_{20}} \tag{13}$$

The total energy contribution ratio of the first j th modes is

$$\gamma_j = \frac{\sum_{k=1}^{j} \overline{E}_k}{\overline{E}_{20}} \tag{14}$$

In order to analyze the participation contributions, 10 nodes are chosen in the cornice, the middle and the ridge of the roof, respectively as shown in Fig. 5. The relationship between mode energy and vibration modes are shown in Fig. 6.

As shown in Fig. 6, the effects of vibration modes on the wind-induced response are different in different positions of the roof structure. For node 1 and node 10 in the cornice of the roof, the important vibration modes are 5th, 9th, 12th and 18th modes and the corresponding average participation ratios are 13.7%, 14.2%, 58.7% and 8.1%, respectively. For the first 12th modes, the average value of the total participation ratios of vibration energy can reach 90.1%, and that of the first 18th modes can reach 100%. For nodes 5 and 6 in the ridge of the roof, the 2nd mode is the dominant mode and the participation ratio of vibration energy is 97.1%. For the first 12th modes, the total participation ratio of vibration energy can reach 100%.

For nodes 3 and 8 in the middle of the cornice and ridge, the 2nd mode is the dominant mode and its energy contribution ratio is 95.6%. The total participation ratio of vibration energy can reach 99.5%. For nodes 2 and 9 near the cornice of the roof, the 5th mode is the dominant mode, and its average energy contribution is 99.6%. For the first 5th modes, the total mode energy can achieve 99.8%. For nodes 4 and node 7 near the ridge of the roof, the 2nd mode is the dominant mode, and its average energy contribution is 95.3%. For the first 9th modes, the total mode energy can achieve 100%.

From above, near the cornice of the roof, the participation of vibration modes is relatively simple. Only considering the first 5th modes, even the first 2nd modes, can reflect the wind-

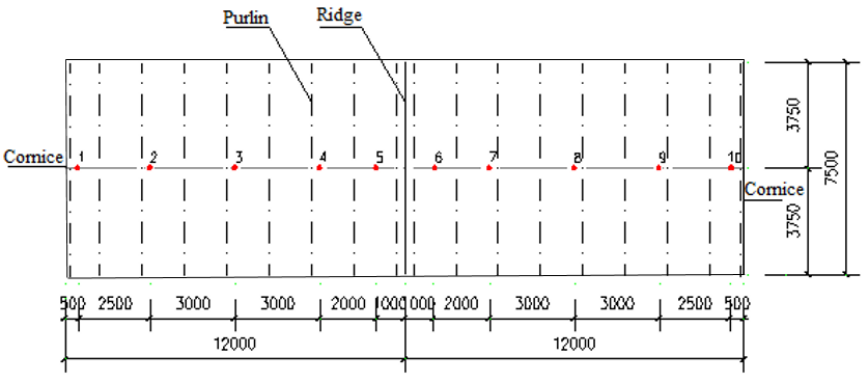

Fig. 5 Distributions of nodes on the roof (Unit: mm)

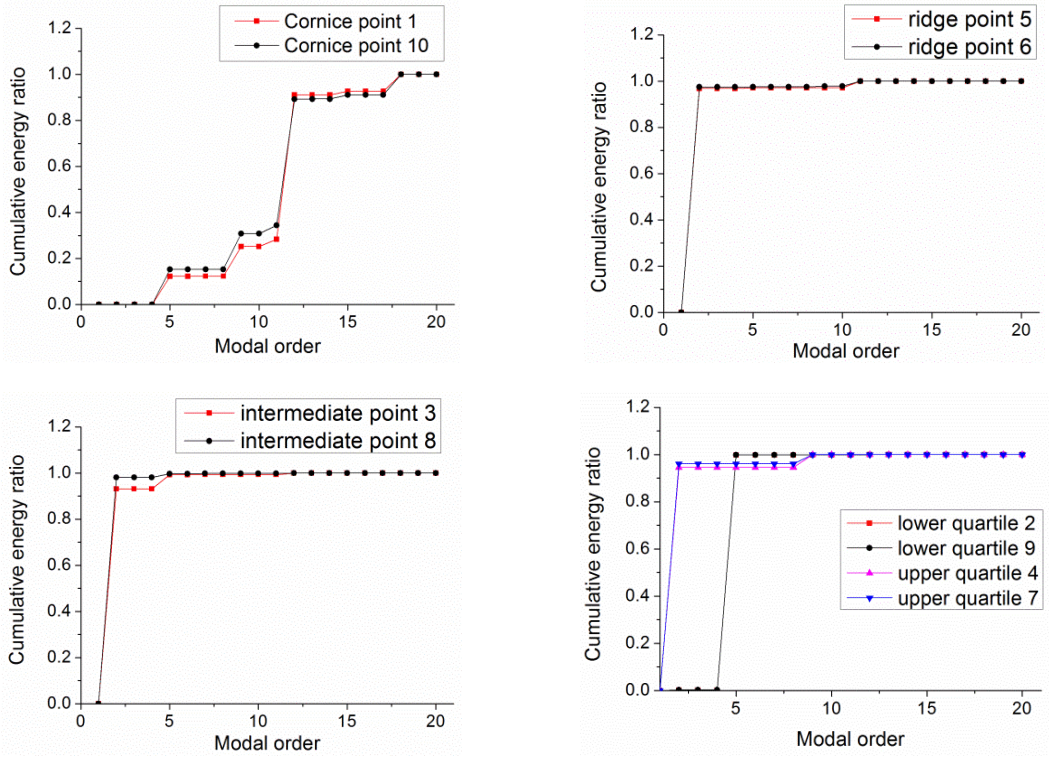

Fig. 6 Relationship between the cumulative energy ratios and the modal orders

induced response. In the roof near the cornice, the participation ratios of vibration modes is relatively complex, and the accurate wind-induced response cannot obtained by only considering the first several modes. Therefore, it may require considering the first 12th even the first 18th orders to accurately calculate the wind-induced structural response.

3.3 The wind-induced vibration coefficient based on the random vibration theories

On the basic of the displacement response y_{ji} in node i, the wind-induced vibration force of mode j for node i can be obtained, called as the equivalent inertia force

$$P_{fji} = M_i \omega_j^2 \mu\sigma_{yji} = M_i \omega_j^2 y_{ji} \tag{15}$$

The wind force of node i is

$$w_i = \beta_i w_{si} = \beta_i \mu_{si} \mu_{zi} w_0 \tag{16}$$

where, ω_0 is the basic wind pressure, ω_{si} is the mean wind pressure of node i, β_i is the wind-induced vibration coefficient of node i, μ_{si} is the shape coefficient of node i, μ_{zi} is the height coefficient of wind pressure of node i. Therefore, the wind-induced vibration coefficient is obtained as follows.

$$\beta_i = \frac{P_{si} + P_{fi}}{P_{si}} = 1 + \sum_{j=1}^{n} \frac{M_i \omega_j^2 y_{ji}}{\mu_{si} \mu_{zi} w_0 A_i} \tag{17}$$

The wind-induced vibration coefficient of the roof structure can be obtained according to Eq. 17. The ground roughness is type B, and the wind height variation coefficient μ_{st} is obtained according to GB 50009-2012 (2012). The wind-induced vibration coefficient distribution of the roof is shown in Fig. 7.

Fig. 7 shows the distribution of wind-induced vibration coefficient on the windward side (right side) and leeward (left side) of the roof is similar, while the wind-induced vibration coefficient in windward side is higher than that of the leeward. The maximum coefficient on the windward side appears near the cornice and the ridge, about 1.37. The maximum coefficient in the leeward near the ridge and cornice is also high, about 1.28.

For the general cantilever structure, for example, high-rise building, tower and chimney etc, the 1st mode is always the dominate mode. Its wind-induced vibration coefficient can be obtained by only considering the effects of the 1st mode.

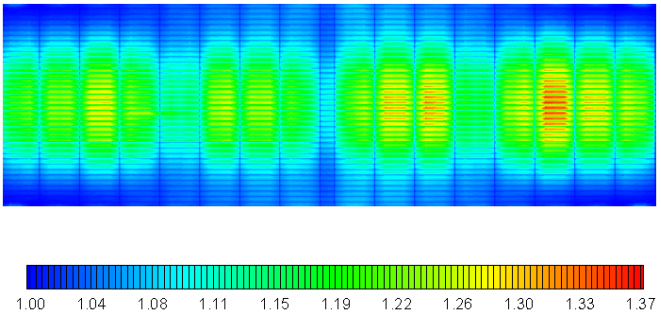

(a) Plane view

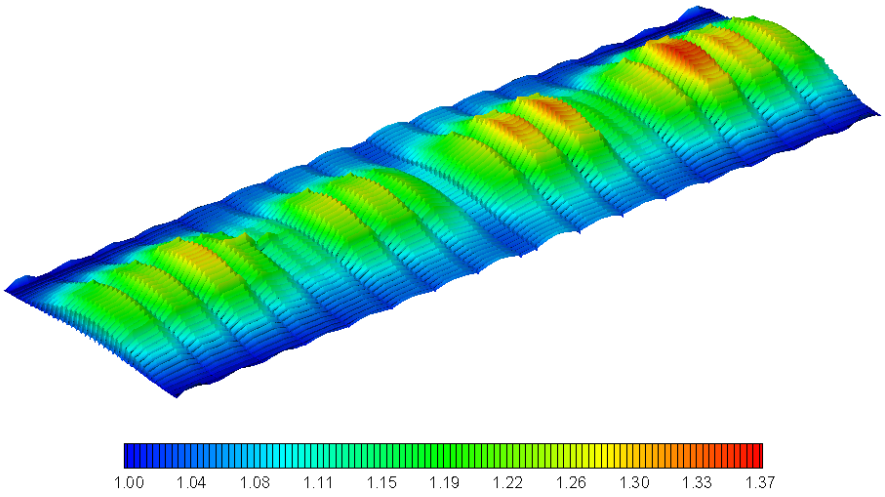

(b) Three-dimensional view

Fig. 7 Distributions of wind vibration coefficient

$$\beta_z = 1 + \frac{\xi \nu \varphi_z}{\mu_z} \tag{18}$$

From above, in the part near the ridge, the participation ratio of vibration modes is very complex, and only considering the first several modes can not reflect the real vibration response of the structures. Then, it is not suitable to use Eq.18 to calculate the wind-induced vibration coefficient of purlin-sheet roof. According to Pei (2009), the proposed wind-induced vibration coefficient of the airport roof with the span of 72-150m is between 1.426 and 1.535. Finally, after comprehensive consideration, the proposed wind-induced vibration coefficient for the general purlin-sheet roof is 1.5.

4. Conclusions

This paper aims to use the random vibration theory to analyze dynamic characteristics and wind vibration coefficients of the purlin-sheet roof. The following conclusions are obtained.

(1) Due to light weight, large flexibility and small damping, the natural vibration frequency of purlin-sheet roof is low and the frequencies and mode distributions are very intensive. Then, the wind vibration response of the roof structure is very complex and the random vibration theory should be employed to analyze the dynamic characteristics of the purlin-sheet roof. Among the first 20th vibration modes, the 1st mode is the deformations of purlins, while all the rest are the overall deformations of the roof. In the following 30th modes, the main modes are unilateral local deformations of the roof. The frequency distribution of the first 20th modes differs significantly, while those of the following 30th modes are relatively similar.

(2) For different parts, the contributions of vibration modes on the vibration response are different. For the part far from the ridge, only considering the first 5th modes, even the first 2nd modes, can accurately reflect the wind-induced vibration response of the structures. For the part near the ridge, only considering the first several modes can not accurately reflect the wind vibration response of the structure. At least the first 12th modes, even the first 18th modes should be considered in the analysis.

(3) For purlin-sheet roof, the distributions of wind vibration coefficient for the upwind and leeward sides are similar, while the first is higher than the latter. The wind vibration coefficient of the upwind surface near the ridge and cornice is the highest, about 1.37. Based on the existing references, the wind vibration coefficient 1.5 is recommended for the design of the general purlin-sheet roof.

Acknowledgments

The research described in this paper was financially supported by the Fundamental Research Funds for the Central Universities (2015QNA57).

References

Ahmad, S. and Kumar, K. (2002), "Effect of geometry on wind pressures on low-rise hip roof buildings", *J. Wind Eng. Ind. Aerod.*, **90**(7), 755-779.

Cai, J.G., Feng, J., Xu, Y.X. and Wang, K. (2013a), "Investigation of the static and dynamic behavior of a deployable hybrid grid shell", *Adv. Struct. Eng.*, **16**(6), 1103-1111.
Cai, J.G., Gu, L.M., Xu, Y.X. Feng, J. and Zhang, J. (2013b), "Non-linear stability analysis of hybrid grid shells", *Int. J. Struct. Stab. Dy.*, **13**(1), Paper No. 1350006.
Cai, J.G., Xu, Y.X., Feng, J. and Zhang, J. (2013c), "Design and analysis of a glass roof structure", *Struct. Des. Tall Spec.*, **22**(8), 677-686.
Cai, J.G., Zhou, Y., Xu, Y.X. and Feng, J. (2013d), "Non-linear stability analysis of a hybrid barrel vault roof", *Steel Compos. Struct.*, *Int. J.*, **14**(6), 571-586.
Cai, J.G., Chao, J., Deng, X.W., Feng, J. and Xu, Y. (2015), "Static analysis of a radially retractable hybrid grid shell in the closed position", *Steel Compos. Struct.*, *Int. J.*, **18**(6), 1391-1404.
Cope, A.D., Gurley, K.R., Gioffre, M. and Reinhold, T.A. (2005), "Low-rise gable roof wind loads: Characterization and stochastic simulation", *J. Wind Eng. Ind. Aerod.*, **93**(9), 719-738.
Davenport, A.G. (1967), "Gust loading factors", *J. Struct. Div.*, **93**(3), 11-34.
Farquhar, S., Kopp, G.A. and Surry, D. (2005), "Wind tunnel and uniform pressure tests of a standing seam metal roof model", *J. Struct. Eng.*, **131**(4), 650-659.
Fu, J., Zhao, R., Xu, A. and Wu, J.R. (2010), "Wind tunnel and full-scale study of wind effects on a large roof structure", *J. Hunan Univ.* (*Nat. Sci.*), **37**(9), 12-18
GB50009-2012 (2012), Load code for the design of building structures; China Architecture & Building Press, Beijing, China.
Ginger, J.D. (2004), "Fluctuating wind loads across gable-end buildings with planar and curved roofs", *Wind Struct.*, *Int. J.*, **7**(6), 359-372.
Habte, F., Mooneghi, M.A., Chowdhury, A.G. and Irwin, P. (2015), "Full-scale testing to evaluate the performance of standing seam metal roofs under simulated wind loading", *Eng. Struct.*, **105**, 231-248.
Huang, B.C. and Wang, C.J. (2008), *Principle and Application of Structural Wind Resistance Analysis*, Tongji University Press, Shanghai, China.
Jacklin, R.B., El Damatty, A.A. and Dessouki, A.A. (2014), "Finite-element modeling of a light-framed wood roof structure", *Wind Struct.*, *Int. J.*, **19**(6), 603-621.
Jubayer, C.M. and Hangan, H. (2014), "Numerical simulation of wind effects on a stand-alone ground mounted photovoltaic (PV) system", *J. Wind Eng. Ind. Aerod.*, **134**, 56-64.
Kasperski, M. (2009), "Specification of the design wind load—A critical review of code concepts", *J. Wind Eng. Ind. Aerod.*, **97**(7), 335-357.
Krentowski, J. (2014), "Steel roofing disaster and the effect of the failure of butt joints", *Eng. Fail Anal.*, **45**, 245-251.
Li, Y.Q. and Dong, S.L. (2001), "Random wind load simulation and computer program for large-span spatial structures", *Spatial Struct.*, **7**(3), 3-11.
Lin, J.X., Surry, D. and Tieleman, H.W. (1995), "The distribution of pressure near roof corners of flat roof low buildings", *J. Wind Eng. Ind. Aerod.*, **56**(2), 235-265.
Liu, M., Chen, X.Z. and Yang, Q.S. (2016), "Characteristics of dynamic pressures on a saddle type roof in various boundary layer flow", *J. Wind Eng. Ind. Aerod.*, **150**, 1-14.
Lou, W., Li, B. and Lu, F. (2002), "Fitting formula to wind pressure distribution on long-span roofs and wind load suggestion", *J. Tongji Univ.*, **30**(5), 588-593.
Lovisa, A.C., Wang, V.Z., Henderson, D.J. and Ginger, J.D. (2013), "Development and validation of a numerical model for steel roof cladding subject to static uplift loads", *Wind Struct.*, *Int. J.*, **17**(5), 495-513.
Lu, F., Lou, W.J. and Sun, B.N. (2002), "Wind-induced dynamic response and wind load factor for long-span flat roof structures", *Eng. Mech.*, **19**(2), 52-57.
Martins, N.E., Martin, P.B. and Baskaran, A. (2016), "Application of statistical models to predict roof edge suctions based on wind speed", *J. Wind Eng. Ind. Aerod.*, **150**, 42-53.
Nakayama, M., Sasaki, Y., Masuda, K., Ogawa, T. (1998), "An efficient method for selection of vibration modes contributory to wind response on dome-like roofs", *J. Wind Eng. Ind. Aerod.*, **73**(1), 31-43.
Pei, Y.Z. (2009), *Research on Wind Loads and Wind-induced Responses of Large-span Aircraft Maintenance Hangars*, Tsinghua University, Beijing, China.

Ren, C., Zhao, X.Z. and Chen, Y.Y. (2016), "Buckling behaviour of partially restrained cold-formed steel zed purlins subjected to transverse distributed uplift loading", *Eng. Struct.*, **114**, 14-24.
Robertson, A., Hoxey, R., Short, J., Ferguson, W.A. and Blackmore, P.A. (1998), "Prediction of structural loads from fluctuating wind pressures: Validation from full-scale force and pressure measurements", *J. Wind Eng. Ind. Aerod.*, **74**(2), 631-640.
Shu, X.L. and Zhou, D. (2003), "AR model of wind speed time series and its rapid implementation", *Spatial Struct.*, **9**(4), 27-32.
Sun, X., Lin, B., Wu, X., Sun, X.Y., Lin, B., Wu, X.R., Wu, Y. and Shen, S.Z. (2008), "Application of numerical wind tunnel to simulate wind load on long-span roof", *Build. Struct.*, **38**(10), 83-86.
Surry, D., Sinno, R.R., Nail, B., Ho, T., Farquhar, S. and Kopp, G. (2007), "Structurally effective static wind loads for roof panels", *J. Struct. Eng.*, **133**(6), 871-885.
Tamura, T. (1999), "Reliability on CFD estimation for wind-structure interaction problems", *J. Wind Eng. Ind. Aerod.*, **81**(1-3), 117-143.
Tieleman, H.W., Surry, D. and Lin, J.X. (1994), "Characteristics of mean and fluctuating pressure coefficients under corner (delta wing) vortices", *J. Wind Eng. Ind. Aerod.*, **52**, 263-275.
Uematsu, Y., Watanabe, K., Sasaki, A., Yamada, M. and Hongo, T. (1999), "Wind-induced dynamic response and resultant load estimation of a circular flat roof", *J. Wind Eng. Ind. Aerod.*, **83**(1), 251-261.
Uematsu, Y., Yamada, M. and Karasu, A. (1997), "Design wind loads for structural frames of flat long-span roofs: Gust loading factor for the beams supporting roofs", *J. Wind Eng. Ind. Aerod.*, **66**(1), 35-50.
Xu, A., Fu, J.Y., Zhao, R.H. and Wu, J.R. (2010), "Field measurements of typhoons according to civil engineering research", *Acta Aerodynamica Sinica*, **28**(1), 23-31.
Yuan, W.B., Cheng, S.S. and Li, L.Y. (2014), "Web-flange distortional buckling of partially restrained cold-formed steel purlins under uplift loading", *Int. J. Mech. Sci.*, **89**, 476-481.
Zhang, X.T. (2006), *Structural Wind Engineering*, China Architecture and Building Press, Beijing, China.
Zhang, L. and Tong, G.S. (2016), "Lateral buckling of simply supported C- and Z-section purlins with top flange horizontally restrained", *Thin-Wall. Struct.*, **99**, 155-167.
Zhou, W., Chen, Y., Peng, B., Yahg, H., Yu, H., Liu, H. and He, X. (2014), "Air damping analysis in comb microaccelerometer", *Adv. Mech. Eng.*, **2014**, Article ID 373172, 6 p.
Zhou, W., Yu, H.J., Zeng, J., Peng, B., Zeng, Z., He, X. and Liu, Y. (2015), "Improving the dynamic performance of capacitive micro-accelerometer through electrical damping", *Microsyst. Technol.*, **22**(12), 2961-2969. DOI: 10.1007/s00542-015-2694-1
Zhu, J., Chen, J.K. and Ren, C. (2014), "Numerical study on the moment capacity of zed-section purlins under uplift loading", *Struct. Eng. Mech., Int. J.*, **49**(2), 147-161.

CC